

## 10-Gb/s Lasercom Terminal for Satellites

Hamid Hemmati and Joseph M. Kovalik  
*Jet Propulsion Laboratory, California Institute of Technology, Pasadena, CA 91109, USA*

**Abstract — Progress in the development and airplane testing of a highly compact, low-mass, low-power consumption, 10-Gb/s laser communications terminal is reported. This terminal is intended for use with Earth-orbiting spacecraft. Design approach, concept of operation, and results of laboratory and field tests are summarized.**

### I. Introduction

This work is motivated by the communications bandwidth requirements anticipated for NASA's future Earth-observing spacecraft. Several of the 17 NASA decadal survey spacecraft (e.g., Advanced Composition Explorer [ACE], Hyperspectral Infrared Imager [HispIRI], and Deformation, Ecosystem Structure, and Dynamics of Ice [DESDynI]) are estimated to require instantaneous downlink data rates from 1 to 9 Gb/s [1]. This requirement is challenging for conventional RF flight and ground subsystems to manage because of spectrum allocation restrictions, among other reasons. Laser communications (lasercom) can deliver multi-Gb/s data rates, while avoiding spectrum allocation issues [2].

The flight subsystem's primary design drivers were day and night communications under diverse atmospheric and link conditions; wavelength-multiplexed communications channels, each up to 2.5-Gb/s data rate; beacon acquisition and fine-pointing for the downlink laser under a generic host platform disturbance; and launch survival to space and the low Earth orbit (LEO) space environment.

The ground subsystem's design drivers include downlink reception from the space terminal at data rates varying from 10 Mb/s to 10 Gb/s; de-multiplex of four communication channels; delivery of a laser beacon to the flight terminal to guide the downlink beam; and downlink processing, including streaming display of telemetry.

Examples of strategies applied to reduce flight subsystem complexity include:

- Multiplexing four lower-data-rate channels to achieve 10-Gb/s downlink, thereby reducing power and complexity of lasers and introducing redundancy, and increasing the ground detector diameter.
- Simplified optical system assembly using a common aperture for transmit and receive.
- Leveraging asymmetrical data rate requirement to simplify design of the flight transceiver by eliminating the need for an uplink data receive channel. The acquisition sensor is used primarily for beacon tracking with capability to receive low-rate (kb/s) commands.
- Taking advantage of the high gain provided by an existing 1-m-diameter ground station, allowing spacecraft transmitter power and aperture size to be reduced. A monostatic ground terminal optics design (in which the same aperture transmits a beacon to the spacecraft and receives the signal) helps to adequately discriminate the weak spacecraft signal from the scattered beacon light. Nearly 117 dB of isolation between two closely spaced wavelengths (1550 nm downlink and 1568 nm beacon) was demonstrated earlier in this ground station.

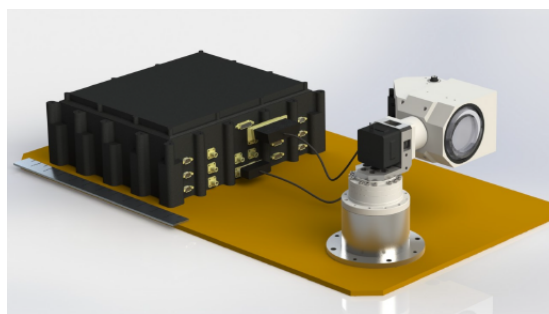


**Fig.1.** Flight terminal assembly including an electronics/laser assembly and an optomechanics/gimbal assembly.

This highly compact flight terminal consists of an optics assembly and an electronics assembly (Fig. 1). The optomechanics assembly is composed of a 5-cm-diameter telescope, a fine-pointing mirror, and a tracking detector mounted together on a precision two-axis gimbal. The electronics assembly houses the laser transmitter; a digital board that functions as processor, modem, and data storage; an analog board for driving the fine-pointing mirror, gimbal, and tracking detector readout; and a power-conditioning

slice. The laser signal is fed into the optical head via a single-mode fiber (output of the fiber amplifier).

## II. Link Analysis

The optical communication link analysis is summarized in Table 1. A 5-cm-diameter aperture transmitting 0.5 W per channel of 1550-nm laser power is received with a 1-m-diameter ground telescope. Link margins shown are for an uncoded bit-error rate (BER) of  $1E-12$ , on-off keying (OOK) modulation, at a data rate of 2.5 Gb/s from 1350 km and 2000 km.

Turbulence with a 3-cm  $r_0$  (Fried parameter) measured at zenith and at 500 nm, and (cloud-free line-of-sight) zenith transmission of 0.9 at 1550 nm, was assumed to represent worst-case atmospheric conditions. Additive background noise from sky radiance and stray light are filtered with a 20-nm noise-equivalent-bandwidth spectral filter.

The point design assumes an elevation angle of  $15^\circ$ . The transmit efficiency loss includes optical transmission and wavefront error losses. The pointing loss presumes a peak mispoint angle (3-sigma jitter plus bias) of 16  $\mu$ rad. The receive telescope efficiency includes optical losses, extinction ratio loss, focused-spot-blurring loss and acquisition/ tracking split, and receiver implementation losses.

When the spacecraft is at zenith, link margin improves to 9 dB. The required power value used in link analysis is inferred from uncoded BER measurements at 1.25 Gb/s.

Incorporating forward error-correction (FEC) codes is expected to increase link margin by an additional 3 dB.

**Table 1.** Link analysis summary for the 10-Gb/s lasercom link.

Average Power	-3 dBW
Transmitter Gain	99.22 dB
Transmitter Efficiency	-2.23 dB
Pointing Loss	-2.27 dB
Range Loss	-264.07 dB
Atmospheric Loss	-1.74 dB
Receive Telescope Gain	125.96 dB
Receive Telescope Effic.	-9.51 dB
Received Signal Power	-57.65 dBW
Required Power	-62.28 dBW
<b>Link Margin</b>	<b>4.6 dB</b>

## III. Concept of Operations

Other assumptions include satellite range to Earth is 200 to 2000 km; data will be generated onboard at a rate of  $\sim 20$  Tb/day and transmitted to ground at the rate of 10 Gb/s at above  $20^\circ$  elevation; data will be transmitted once per orbit with greater than 60% probability (of clear atmosphere) per ground station; there will be sufficient onboard data storage commensurate with the number of available ground terminals; given cloud-free line of sight, the entire buffer will be emptied in one pass; and the average contact time with the ground station is 3 to 8 minutes.

The concept of operations includes:

- A spacecraft pass is scheduled ahead of time for each ground station. Link budgets based on the specific atmospheric and orbit conditions at the time of operation determine the data rates to be applied. This information is passed to the satellite ahead of time.
- Based on prior knowledge of the satellite ephemeris, the ground terminal in the queue blind-points a laser beacon towards the satellite location.
- Based on orbital position knowledge, and with the aid of a two-axis gimbal, the flight optical terminal coarse-points to the ground terminal.
- If the flight terminal successfully acquires the uplink beacon, both flight and ground terminals track each other. The flight terminal then fine-points its outgoing laser beam and transmits data to the ground terminal.
- If the flight terminal does not successfully acquire the uplink beacon in  $<5$  s, then through a prespecified range of conical scans the flight terminal will acquire the uplink beacon in  $<10$  s.
- Point-ahead will be implemented via the fast-steering mirror.
- If the uplink beacon signal or the downlink data reception is interrupted, the initial acquisition procedure is repeated.
- In case of adverse change in the atmospheric conditions, the pass may have to be terminated.
- The ground terminal monitors the incoming data to determine whether the operation is proceeding successfully. Enough data will be sampled to notify the satellite whether it should empty the buffer.

- Received data are stored for subsequent processing.

The communications link continues until the pass is over. If the link is interrupted at any point, the spacecraft restarts the acquisition procedure.

#### IV. Flight Terminal

##### *Downlink Flight Laser Transmitter*

The downlink data rate of 10 Gb/s is achieved by multiplexing four channels of 2.5-Gb/s data at wavelengths separated by ~5 nm. A total of 2 W of average laser power is required from a slant range of 1300–2000 km to deliver 10 Gb/s from LEO to Earth.

Four directly modulated and temperature-controlled distributed feedback (DFB) diode lasers with wavelengths within the C-band of an erbium-doped fiber amplifier (EDFA) are wavelength-multiplexed. Seed laser assembly dimensions are 15 cm x 12.5 cm x 2 cm (Fig. 2).

The modulation extinction ratio for each laser is ~12 dB. The four output ports of the seed laser assembly are connected to the four input channels of a highly compact (10.7 cm x 7 cm x 2 cm), C-band, fiber amplifier (Fig. 3). The thermally managed transmit laser, housed in the electronics assembly, connects to the optical head via an optical fiber (Fig. 1).



**Fig. 2.** The four-channel seed laser consisting of four DFB lasers, each modulated directly at 2.5 Gb/s.



**Fig. 3.** The 2-W, C-band, ruggedized commercial fiber amplifier.

##### *Flight Optics Assembly*

We developed three different design configurations of compact 5-cm-diameter telescopes. These include all-refractive optics, all-reflective optics with off-axis parabola, and a monolithic refractive/reflective optics design. Their properties differ in terms of overall throughput, aberrations, ability to mitigate background light, and overall volume.

The flight telescope transmits four multiplexed laser beams (with wavelengths centered around 1550 nm) to the ground, and receives 1568-nm laser signal from the ground.

Laser beacon tracking using the ground-supplied beacon signal falls on an InGaAs quadrant detector within the optical assembly. This array serves as the large ( $\pm 2$  mrad) field of view acquisition sensor to accommodate platform pointing of ~2 mrad. A fine-tracking error signal inferred from the quad detector is fed to a fine-pointing mirror to reduce the peak-to-peak pointing error to less than 10  $\mu$ rads.

A 20-nm-wide spectral filter in front of the quadrant detector suppresses upwelling daytime background noise. The uplink beacon is modulated at greater than 10 kHz. This suppresses background and scatter from the high-power downlink. The footprint of the downlink beam on the ground varies from 100 to 150 m depending upon range. Fig. 4 shows a picture of the optomechanics assembly based on the refractive optics design.

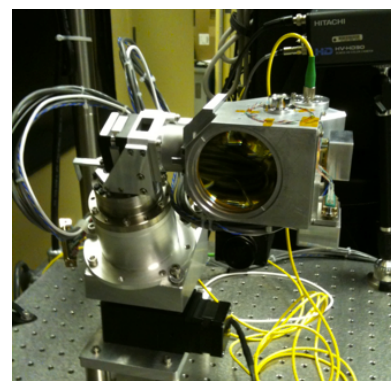


**Fig. 4.** Prototyped optical head including the optics assembly and two-axis gimbal.

##### *Modem and Electronics Assembly*

An electronics assembly composed of modems, controllers, processors, memory, and power-conversion electronics was developed based on flight-grade parts.

The digital board features a Xilinx V to support the transceiver at data rates of 10 Gb/s (Fig. 5). The analog board containing the fine-pointing mirror controller and detector array readout electronics was also developed based on flight-grade electronics (Fig. 6).



**Fig. 5.** Digital electronics board containing modems, processors, and memory, capable of supporting 10-Gb/s data rate. Developed based on flight-grade parts.

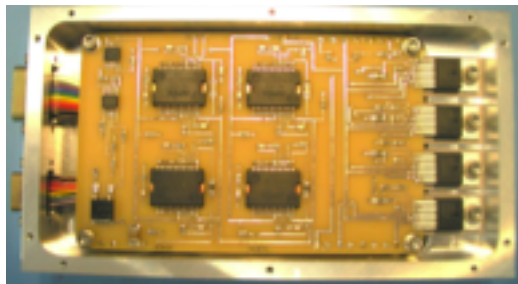


**Fig. 6.** Analog electronics slice. Its primary functions are to drive and control the fine-pointing mirror and to read out the quadrant detector.

#### *Coarse-Pointing Gimbal*

The optics assembly is located on a high-precision, compact, two-axis gimbal for initial (coarse) blind-pointing.

The gimbal is a two-axis elevation over azimuth system, where each axis is actuated via a stepper motor coupled to a harmonic gear drive. The off-the-shelf components used in gimbal prototype development can be replaced with identical performance flight-qualified parts. The stepper motor detent torque, in combination with harmonic drive static torque and the gear ratio of the harmonic drive, provide sufficient holding torque for the gimbal to immobilize the optical head during spacecraft launch.

For finer motion resolution, the gimbal controller applies continuous drive to the motor coils, rather than the more standard microstepper driver. To move the stepper motor between two steps, sinusoidal current

with 90° phase between the two motor coils is continuously adjusted. The control software monitors the current phase and the number of steps made in order to record the gimbal position. No other encoder or resolver is used. To measure the gimbal transfer function, it was commanded in velocity, while motion of the incoming emulated uplink beacon was recorded on the quad sensor. Transfer functions for the azimuth and elevation axes are dominated by a single resonance that is due to the torsion of the inertial payload about the actuator shaft. The elevation resonance is higher in frequency than that of the azimuth since the azimuth must carry the extra load of the elevation axis (Fig. 7).

Attempts to stiffen the gimbal structure did not raise the resonant frequency. This resonant frequency sets the bandwidth of the control loop for the gimbal servo. The resonance becomes the dominant source of jitter when the stepper motor stepping frequency coincides with it.

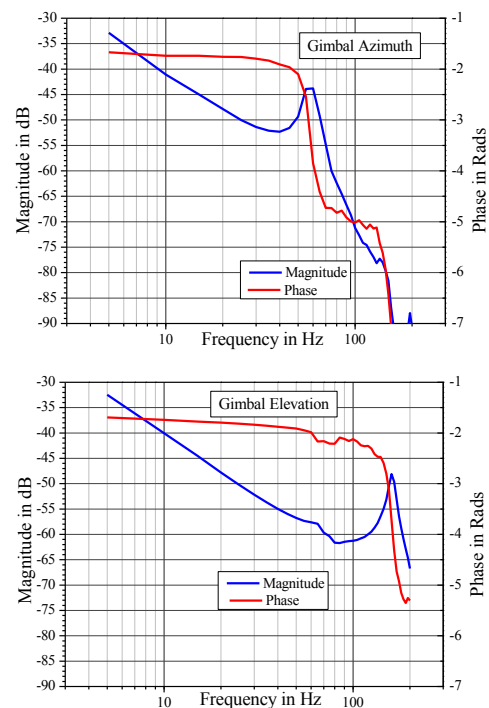


**Fig. 7.** Transfer function of the gimbal azimuth (upper chart), and elevation (lower chart).

To measure gimbal closed-loop jitter, we emulated motion in a laboratory by mounting the gimbal on a wedge that was placed on a rotary stage. The gimbal was actuated at an angular rate similar to that seen in true satellite tracking ( $<2^\circ/s$ ). Closed-loop tracking with an emulated beacon as reference adds the jitter of

the rotary stage to the gimbal jitter (Fig. 8). This provides an upper bound on the gimbal performance. The measurements were made for both the full control loop with the fine-steering mirror and gimbal control, and a partial control loop using only gimbal control at an angular rate of  $1.5^\circ/\text{s}$ .

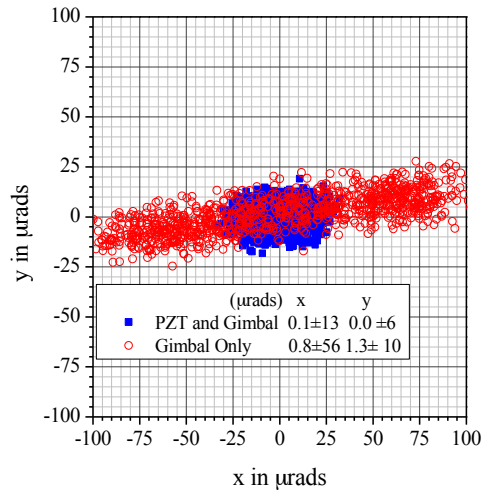


**Fig. 8.** Flight terminal jitters for gimbal-only actuation and gimbal with fine-pointing actuation.

The measured gimbal jitter was found to depend on both the angular rate and the actual azimuth position of the gimbal. The primary source of this jitter is the stepper motor angular noise transmitted through the harmonic drive. Noise levels increase when the stepping frequency approaches the resonant frequency of the gimbal payload on the actuator shaft.

## V. Ground Terminal

The ground system must provide an uplink beacon as well as receive/detect the high-rate downlink data signal. For links from the spacecraft, use of the 1-m-diameter lasercom-dedicated telescope at Wrightwood, California (called the Optical Communications Telescope Laboratory) is planned [3]. This telescope is capable of blind-pointing to an accuracy of  $<20 \mu\text{rad}$  according to a given ephemeris file generated for the specific satellite pass.

For laboratory and field tests (ranges of  $<1 \text{ km}$  for ground-to-ground to  $7 \text{ km}$  for airplane-to-ground), we use a 10-cm refractive telescope or a 30-cm-diameter reflective telescope.

The downlink signal must be separated into its four separate spectral constituents. The incoming light is focused and collimated by two positive lenses or an afocal reflective telescope into a beam a few millimeters wide.

The collimated beam is reflected off a fine-steering mirror. Part of the light is split and sent to an InGaAs quadrant detector. The remaining light goes to the filters that separate the wavelengths.

Four identical filters with a bandwidth less than  $1 \text{ nm}$  and center wavelength longer than the highest wavelength were used. Each filter was angle-tuned for a specific downlink wavelength. After filtering, each channel was re-focused onto a  $75\text{-}\mu\text{m}$  InGaAs avalanche photodiode (APD) for detection and conversion into an electrical signal.

A special-purpose ground gimbal was developed to hold the ground optical receiver system and point it at the prototype flight system. This gimbal uses a fork-mount design. Each actuator is stepper motor coupled to a harmonic gear drive. A standard microstepper driver sources current to each motor. Control software monitors the number of microsteps made in order to record the gimbal position [Fig. 9].



**Fig. 9.** Ground terminal and control electronics.

For end-to-end testing, the ground system can acquire and track moving sources. Both a silicon and InGaAs camera are co-aligned with the ground receiver optical axis. These are used to point the gimbal to a visually identified source like the tracking lights of an airplane. The gimbal can track the airplane in the visible or infrared. Once the downlink beam is visible by the InGaAs camera, it can also be used as a tracking source.

The communications link is established upon detection of the  $1550\text{-nm}$  downlink signal with the InGaAs quad. Nested controls loop with both the fine-steering mirror and gimbal tracks

the incoming downlink beam using quadrant cell signal.

#### *Ground Uplink Laser Transmitter (Beacon and Data)*

The 1568-nm wavelength was assumed for an uplink beacon laser transmitted through the ground telescope. The required uplink laser power depends upon the flight terminal's control-loop bandwidth. For example, a 10-Hz bandwidth requires  $\sim 10$  W of average laser power. A 0.2-milliradian uplink laser beamwidth will cover the position uncertainty of the spacecraft with adequate margin. Operational procedures for conducting safe laser beam uplink typically require advance notice to the Laser Clearing House (LCH).

### **VI. Laboratory and Ground-to-Ground Field Tests**

Emulated signals in the four flight terminal channels consist of a live 1.5-Gb/s, uncompressed, high-definition (HD) video; a recorded 1.5-Gb/s uncompressed HD video; eight digitized and multiplexed analog videos totaling 1.5 Gb/s data rate; and a 2.5-Gb/s pseudorandom binary sequence (PRBS).

A series of laboratory and field tests was performed over a 500-m range and a nearly horizontal path. Initially, this verified the static pointing of each terminal. Since atmospheric beam wander hampers robust links when the downlink beam is only  $50 \mu\text{rad}$  in a horizontal path, attempts to emulate links with dynamic motion provided by rotary stages did not work. Measurements were made for the effective beam jitter and they agreed with calculations of atmospheric beam wander for the conditions used in the experiment. Although this experiment measured the same beam jitter in the many-hundred  $\mu\text{rad}$  range, it can be reduced to the  $10\text{-}\mu\text{rad}$  level by increasing the aperture size, performing the link at dawn or dusk when the atmospheric seeing is optimal, or by going to a link with an elevation greater than  $20^\circ$ .

### **VII. Airplane-to-Ground Links**

The flight terminal prototype was fully integrated with an aircraft for flight test of the acquisition, tracking, and pointing assembly (Fig. 10). To acquire the ground station, the flight terminal uses a commercial inertial measurement unit (IMU) to blind-point to the

ground station location. The IMU is not necessary for spacecraft links since ephemeris knowledge is available through its avionics subsystem. The flight system acquires and tracks on the uplink beacon signal using a camera that is co-aligned with the flight receiver.

To acquire the aircraft from the ground, we use an all-sky camera that incorporates a fisheye lens with a CCD camera. Frame subtraction is applied to the images to identify airplane lights. Once the airplane is identified, coordinates are passed to the gimbal to point to its location. The camera on the gimbal finds the airplane lights, tracks it, and illuminates the aircraft with the beacon.

The tracking control on the flight system is transferred to the quad cell when the uplink beacon is detected. The downlink laser signal should be illuminating the ground system at this point. Two-way, closed-loop tracking occurs following the above procedures.



**Fig. 10.** Flight terminal together with electronics and laser integrated in a Cessna 206 aircraft.

Figures 11 and 12 show data from an airplane-to-ground test. The plane would fly about the ground station at a slant range of 5–7 km and elevation of  $15\text{--}30^\circ$ . The ground terminal could acquire the flight terminal and the flight terminal could track on the uplink beacon. For the initial experimental links from the airplane, the downlink beam was widened to  $300 \mu\text{rad}$ .

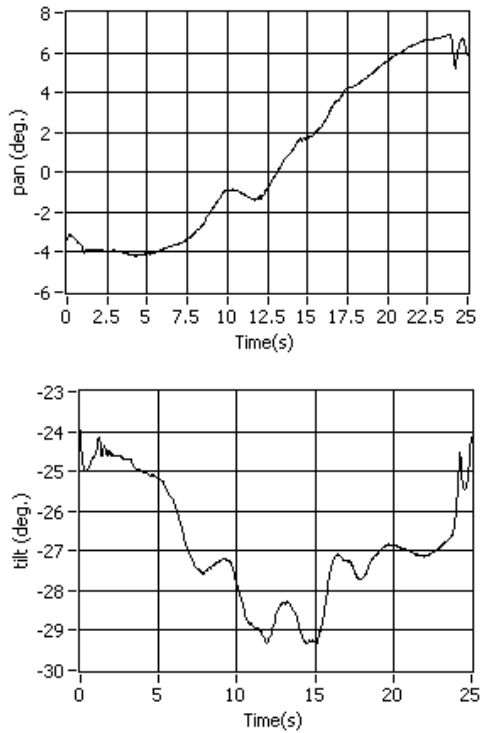


**Fig. 11.** The upper graph shows the flight terminal gimbal pan angle while the lower plot shows the tilt over a period of 25 s while tracking.

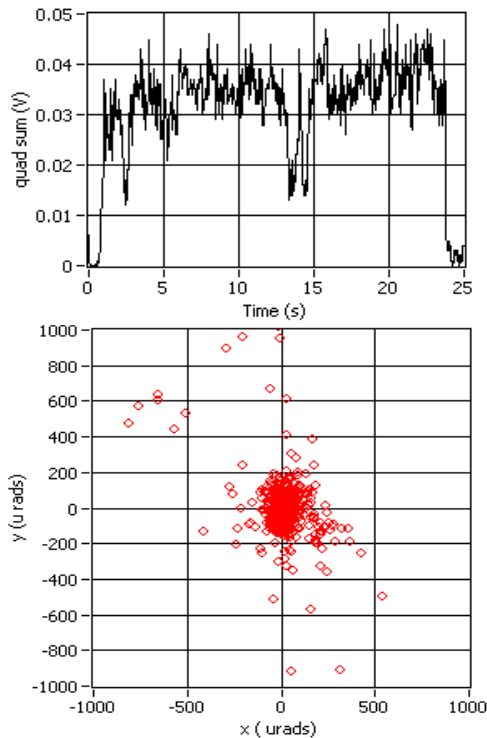


**Fig. 12.** The upper graph shows the light incident on the flight terminal quad detector while the lower plot shows the measured pointing over a period of 25 s while tracking.

In conclusion, JPL is developing a compact lasercom terminal for 10-Gb/s data downlinks from LEO spacecraft. Prototypes of the optomechanics assembly and gimbal for the flight system, as well as the electronics/laser assembly for the flight terminal, were developed and successfully tested. A portable test ground terminal to receive the high-rate downlink and provide an emulated uplink beacon has also been built and tested. The two ends of the link have been tested in a dynamic laboratory environment that emulates the real satellite link with equivalent angular rates of motion. Airplane-to-ground links are ongoing.

The final product of this project will be the realization of a full prototype lasercom terminal that will require minimal further technology development, with no need for flight component development.

#### Acknowledgements

The work described here was performed at the Jet Propulsion Laboratory (JPL), California Institute of Technology, under contract with the National Aeronautics and Space Administration (NASA). The authors are indebted to their colleagues: A. Biswas, T. Roberts, V. Garkanian, C. Explores, J. Gin, and D. Nguyen, who have made valuable contributions to the work reported here.

Copyright to be transferred to IEEE. US Government sponsorship acknowledged.

#### References

1. R. Biswas, J. Dunbar, J. Hardman, F. R. Bailey, L. Wheeler, and S. Rogers, "A Look at the Impact of High-End Computing Technologies on NASA Missions," SPIE Proceedings, 7587, 75870B (2010).
2. A. Freeman, P. Rosen, R. Jordan, W. T. K. Johnson, S. Hensley, T. Sweetser, A. Loverro, J. Smith, G. Sprague, and Y. Shen, "DESDynI — A NASA Mission for Ecosystem, Solid Earth, and Cryosphere Science," SP-668, 4th Int. Workshop on Science and Applications of SAR Instruments, [earth.esa.int/workshops/polinsar2009/.../paper\\_169\\_s1\\_4free.pdf](http://earth.esa.int/workshops/polinsar2009/.../paper_169_s1_4free.pdf)
3. K. E. Wilson, J. Kovalik, A. Biswas, M. Wright, W. T. Roberts, Y. Takayama, and S. Yamakawa, "Preliminary Results of the OCTL to OICETS Optical Link Experiment (ORROLE)," SPIE Proceedings, 7587, (2010).